ARMY RESEARCH LABORATORY

A Yield Strength Model and Thoughts on an Ignition Criterion for a Reactive PTFE-Aluminum Composite

by M. N. Raftenberg, M. J. Scheidler, and D. A. Casem

ARL-RP-219 **August 2008**

A reprint from the *Proceedings of the 55th JANNAF Conference*, Newton, MA, 12–16 May 2008.

NOTICES

Disclaimers

The findings in this report are not to be construed as an official Department of the Army position unless so designated by other authorized documents.

Citation of manufacturer's or trade names does not constitute an official endorsement or approval of the use thereof.

Destroy this report when it is no longer needed. Do not return it to the originator.

Army Research Laboratory
Aberdeen Proving Ground, MD 21005-5069

ARL-RP-219 **August 2008**

A Yield Strength Model and Thoughts on an Ignition Criterion for a Reactive PTFE-Aluminum Composite

M. N. Raftenberg, M. J. Scheidler, and D. A. Casem
Weapons and Materials Research Directorate, ARL

A reprint from the *Proceedings of the 55th JANNAF Conference*, Newton, MA, 12–16 May 2008.

REPORT DOCUMENTATION PAGE

Form Approved
OMB No. 0704-0188

1. REPORT DATE *(DD-MM-YYYY)*	2. REPORT TYPE	3. DATES COVERED (From - To)
August 2008	Reprint	1 October–12 May 2008

4. TITLE AND SUBTITLE
A Yield Strength Model and Thoughts on an Ignition Criterion for a Reactive PTFE-Aluminum Composite

5a. CONTRACT NUMBER

5b. GRANT NUMBER

5c. PROGRAM ELEMENT NUMBER

6. AUTHOR(S)
M. N. Raftenberg, M. J. Scheidler, and D. A. Casem

5d. PROJECT NUMBER
622618H80

5e. TASK NUMBER

5f. WORK UNIT NUMBER

7. PERFORMING ORGANIZATION NAME(S) AND ADDRESS(ES)
U.S. Army Research Laboratory
ATTN: AMSRD-ARL-WM-TD
Aberdeen Proving Ground, MD 21005-5069

8. PERFORMING ORGANIZATION REPORT NUMBER
ARL-RP-219

9. SPONSORING/MONITORING AGENCY NAME(S) AND ADDRESS(ES)

10. SPONSOR/MONITOR'S ACRONYM(S)

11. SPONSOR/MONITOR'S REPORT NUMBER(S)

12. DISTRIBUTION/AVAILABILITY STATEMENT
Approved for public release; distribution is unlimited.

13. SUPPLEMENTARY NOTES
A reprint from the *Proceedings of the 55th JANNAF Conference*, Newton, MA, 12–16 May 2008.

14. ABSTRACT

We studied a pressed and sintered reactive composite of 74 wt% polytetrafluoroethylene (PTFE, or Teflon) and 26 wt% aluminum powder. A model, which we call "JCP", was developed to relate the yield strength of this material to the equivalent plastic strain, total strain rate, and temperature. The model was fit to Instron compression data at 0.1/s strain rate and split Hopkinson pressure bar (SHPB) compression data at approximately 2900/s strain rate. The SHPB database included initial temperatures of 297K and 325K. The model predicted a high susceptibility to shear localization due to the material's thermal softening and strain hardening characteristics. The hypothesis of shear localization as a precursor to ignition led us to consider equivalent plastic strain as a basis for an ignition initiation criterion. The JCP model was installed into the EPIC finite element wavecode and used to simulate Taylor impact tests involving impact speeds of 104 and 222 m/s. The computed boundary shapes versus time were compared with digitized images from a framing camera. Agreement was good at 104 m/s throughout the 36-μs time range of observation. Agreement was good at 222 m/s until 16 μs after impact. Thereafter the photographs displayed a greater degree of mushrooming than did the EPIC simulation. We speculated that internal ignition, fracture of various modes including petalling, and inaccuracies associated with interpolations and extrapolations of our JCP fit all may accounted for some of the mushrooming in excess of that predicted using JCP.

15. SUBJECT TERMS
reactive material, PTFE-aluminum, Teflon, ignition, yield strength

16. SECURITY CLASSIFICATION OF:			17. LIMITATION OF ABSTRACT	18. NUMBER OF PAGES	19a. NAME OF RESPONSIBLE PERSON
a. REPORT	b. ABSTRACT	c. THIS PAGE			M. N. Raftenberg
UNCLASSIFIED	UNCLASSIFIED	UNCLASSIFIED	UL	20	19b. TELEPHONE NUMBER (*Include area code*) 410-278-3684

A YIELD STRENGTH MODEL AND THOUGHTS ON AN IGNITION CRITERION FOR A REACTIVE PTFE-ALUMINUM COMPOSITE

M. N. Raftenberg, M. J. Scheidler, D. A. Casem
U.S. Army Research Laboratory, Aberdeen Proving Ground, MD

ABSTRACT

We studied a pressed and sintered reactive composite of 74 wt% polytetrafluoroethylene (PTFE, or Teflon) and 26 wt% aluminum powder. A model, which we call "JCP", was developed to relate the yield strength of this material to the equivalent plastic strain, total strain rate, and temperature. The model was fit to Instron compression data at 0.1/s strain rate and split Hopkinson pressure bar (SHPB) compression data at approximately 2900/s strain rate. The SHPB database included initial temperatures of 297K and 325K. The model predicted a high susceptibility to shear localization due to the material's thermal softening and strain hardening characteristics. The hypothesis of shear localization as a precursor to ignition led us to consider equivalent plastic strain as a basis for an ignition initiation criterion. The JCP model was installed into the EPIC finite element wavecode and used to simulate Taylor impact tests involving impact speeds of 104 and 222 m/s. The computed boundary shapes versus time were compared with digitized images from a framing camera. Agreement was good at 104 m/s throughout the 36-μs time range of observation. Agreement was good at 222 m/s until 16 μs after impact. Thereafter the photographs displayed a greater degree of mushrooming than did the EPIC simulation. We speculated that internal ignition, fracture of various modes including petalling, and inaccuracies associated with interpolations and extrapolations of our JCP fit all may accounted for some of the mushrooming in excess of that predicted using JCP.

INTRODUCTION

We have studied a pressed and sintered stoichiometric mixture of 74 wt% polytetrafluoroethylene (PTFE, also known as Teflon) and 26 wt% aluminum powder. Typical average pre-sintered particle sizes were 28 and 9 μm for the PTFE and aluminum, respectively. This material, denoted "PTFE-Al", has been found to react in Taylor impact tests at sufficiently high impact speeds.[1, 2] Figure 1 shows impact at 222 m/s of a rod with an initial length of 50.8 mm and diameter of 7.59 mm. A 68-frame Hadland framing camera was used. The steel anvil appears in the lower portion of each photograph, and an aluminum sabot appears in the upper portion. This sabot had a mass of 0.101 kg, an outer diameter of 39.6 mm, and a total length of 30.5 mm, 10.2 mm of which was hollowed out to accommodate the rearmost portion of the PTFE-Al rod. In Figure 1 we see a flash near the mushroomed leading edge of the specimen at 32 μs post impact.

Figure 2 shows a conical PTFE-Al specimen from another Taylor impact test. This test involved an impact speed of 104 m/s. The rod's initial length and diameter were again 50.8 and 7.59 mm, respectively. The flat, circular base of this cone suggests that it coincided with the impact face of the original cylinder. The conical surface shown in Figure 2 displays evidence of ductile flow, and its blackened regions suggest ignition. On the basis of this specimen, we developed a shear localization hypothesis and adopted a metals-like approach to modeling mechanical properties of PTFE-Al, i.e., an equation of state for the dilatational response and von Mises plasticity for the deviatoric response.

Reference 3 presented data from uniaxial compressive-stress tests on PTFE-Al with an Instron machine at a constant true-strain rate of 0.1/s and with a split Hopkinson pressure bar (SHPB) at an approximately constant true-strain rate of about 2900/s. The Instron specimen's initial temperature was 296K. Two SHPB specimens were initially at 297K and two were at 325K. These Instron and SHPB data are collected in Figure 3.

In the present paper we propose a yield strength model which we call "JCP", an explicit function of equivalent plastic strain, equivalent-strain rate, and temperature, that we fit to the data in Figure 3. We

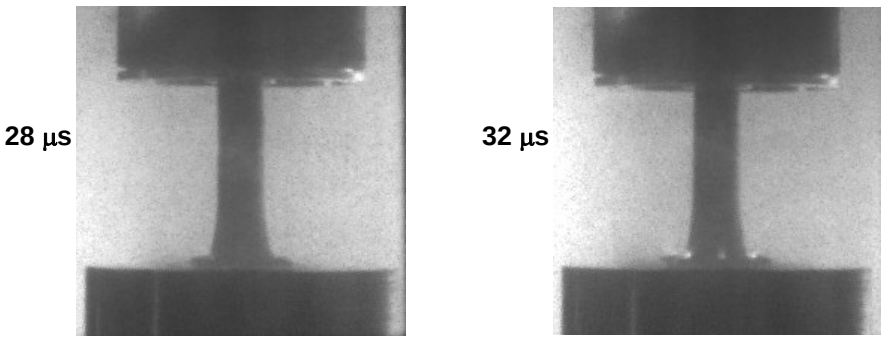

Figure 1. A Taylor impact test shown 28 and 32 μs after initial impact at 222 m/s. The PTFE-Al cylinder's initial length and diameter were 50.8 and 7.59 mm, respectively. Note the steel anvil at the bottom and the aluminum sabot at the top of this photograph. (Reproduced from reference 3.)

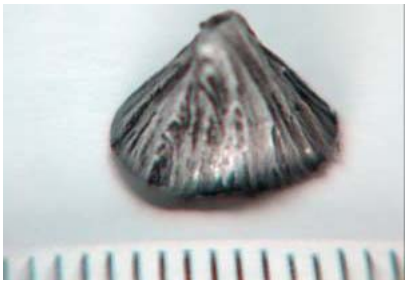

Figure 2. A conical PTFE-Al specimen recovered from a Taylor impact test at 104 m/s. The scale shown is in millimeters. The cylinder's initial length and diameter were 50.8 and 7.59 mm, respectively. (Reproduced from reference 3.)

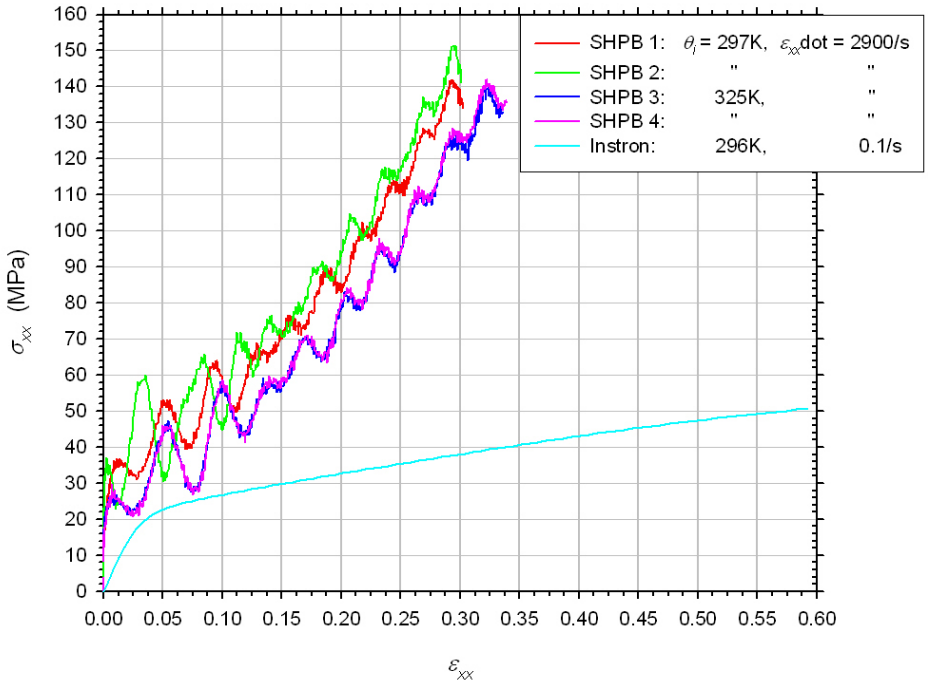

Figure 3. Instron and SHPB Compression Data for PTFE-Al. (Reproduced from reference 3.)

installed this model into the EPIC Lagrangian, finite-element wavecode[4]. We then used EPIC to simulate the Taylor impact tests at 104 and 222 m/s. We compared computed specimen shapes with framing-camera images at specific times post impact. At the higher impact speed, we obtained general agreement with experiment throughout the first 16 μs. Thereafter, JCP under-predicted the extent of specimen mushrooming near the anvil interface. We attributed this discrepancy to one or more of three broad causes: interior ignition, material damage, and deficiencies in our representation of the material's undamaged, inert properties.

In the remainder of the paper, we provide experimental evidence for the damage mechanism known as "petalling". We note the tendency of the JCP model, with its explicit thermal softening, to produce the phenomenon of adiabatic shear localization. We consider the latter's implications for PTFE-Al ignition. We propose a model that can introduce some effects of ignition into an EPIC simulation.

RESULTS AND DISCUSSION

THE JCP YIELD STRENGTH MODEL

We propose the following functional form to represent the constitutive data in Figure 3.

$$\sigma_{\mathrm{JCP}}(\varepsilon^p, \theta, \dot{\varepsilon}) = \left[\hat{A}(\dot{\varepsilon}) + \hat{B}(\dot{\varepsilon}) \cdot (\varepsilon^p)^{\hat{N}(\dot{\varepsilon})}\right]\left(\frac{\theta_m - \theta}{\theta_m - 294\mathrm{K}}\right) \tag{1}$$

where

$$\hat{A}(\dot{\varepsilon}) = A_0 + A_1 \sinh^{-1}\left(\dot{\varepsilon}/2\dot{\varepsilon}_0\right) \tag{2a}$$

$$\hat{B}(\dot{\varepsilon}) = B_0 \left(B_1\right)^{\hat{N}(\dot{\varepsilon})} \tag{2b}$$

$$\hat{N}(\dot{\varepsilon}) = N_0 + N_1 \sinh^{-1}\left(\dot{\varepsilon}/2\dot{\varepsilon}_0\right) \tag{2c}$$

Here, the von Mises effective stress, σ, is an explicit function of equivalent plastic strain, ε^p, the total equivalent-strain rate, $\dot{\varepsilon}$, and the absolute temperature, θ. The model introduces seven material constants: A_0, A_1, B_0, B_1, N_0, N_1, and θ_m., plus the normalizing strain rate, $\dot{\varepsilon}_0$.

In equation 1 thermal softening is multiplicatively decoupled from strain hardening and strain-rate hardening. The material constant θ_m is the parameter governing thermal softening and is the temperature corresponding to zero strength. Note that equation 1 cannot be used when θ exceeds θ_m.

In equation 1, $\hat{A}$ and $\hat{C}$ are two independent functions of total equivalent-strain rate $\dot{\varepsilon}$. The inverse hyperbolic sine function that governs the strain-rate dependence is related to the logarithm function by the identity

$$\sinh^{-1}\left(\frac{\dot{\varepsilon}}{2\dot{\varepsilon}_0}\right) = \ln\left[\frac{\dot{\varepsilon}}{2\dot{\varepsilon}_0} + \sqrt{\left(\frac{\dot{\varepsilon}}{2\dot{\varepsilon}_0}\right)^2 + 1}\right] \tag{3}$$

JCP AND A CONSTANT-STRAIN-RATE, CONSTANT-DENSITY, ADIABATIC PROCESS

Suppose a JCP material undergoes a thermodynamic process that is adiabatic and involves constant strain rate $\dot{\varepsilon}_*$. The first law of thermodynamics can be used to derive a one-to-one mapping between temperature and equivalent plastic strain. During plastic strain increment $d\varepsilon^p$, the increment in plastic work per unit mass is

$$dw^p = \sigma_{\mathrm{JCP}}(\varepsilon^p, \theta, \dot{\varepsilon}_*)\, d\varepsilon^p$$

Assume that any work associated with elastic deformation, whether dilatational or elastic deviatoric, is relatively negligible. Assume that density remains approximately constant during the process, so that the change in internal energy per unit mass is

$$de = \rho_0 c_v d\theta$$

where c_v is the specific heat at constant volume. Assume that the Taylor-Quinney factor is nearly 1, so that nearly all plastic work is converted into heat. The first law of thermodynamics then requires that

$$\rho_0 c_v d\theta = \sigma_{\mathrm{JCP}}(\varepsilon^p, \theta, \dot{\varepsilon}_*)\, d\varepsilon^p \tag{4}$$

Combining equations (1) and (4),

$$\int_{\theta_i}^{\theta_{JCP}^{adiab}} \frac{d\theta}{\theta_m - \theta} = \frac{1}{\rho_0 c_v (\theta_m - 294K)} \int_0^{\varepsilon^p} \left[\hat{A}(\dot{\varepsilon}_*) + \hat{B}(\dot{\varepsilon}_*) \times (\varepsilon^p)^{\hat{N}(\dot{\varepsilon}_*)} \right] d\varepsilon^p$$

Here θ_i is the initial temperature. The result is

$$\theta_{\mathrm{JCP}}^{\mathrm{adiab}}(\varepsilon^p, \dot{\varepsilon}_*) = \theta_m + (\theta_i - \theta_m) \cdot \exp\left[-\phi(\varepsilon^p, \dot{\varepsilon}_*) \right] \tag{5}$$

The result for stress in the material governed by equation 1 during an adiabatic, constant-density, constant-strain-rate process is

$$\sigma_{\mathrm{JCP}}^{\mathrm{adiab}}(\varepsilon^p, \dot{\varepsilon}_*) = \left(\frac{\theta_m - \theta_i}{\theta_m - 294\mathrm{K}} \right) \cdot \left[\hat{A}(\dot{\varepsilon}_*) + \hat{B}(\dot{\varepsilon}_*) \cdot (\varepsilon^p)^{\hat{N}(\dot{\varepsilon}_*)} \right] \cdot \exp\left[-\phi(\varepsilon^p, \dot{\varepsilon}_*) \right] \tag{6}$$

where

$$\phi(\varepsilon^p, \dot{\varepsilon}_*) = \frac{1}{\rho_0 c_v (\theta_m - 294\mathrm{K})} \cdot \left[\hat{A}(\dot{\varepsilon}_*) \cdot \varepsilon^p + \frac{\hat{B}(\dot{\varepsilon}_*)}{\hat{N}(\dot{\varepsilon}_*) + 1} \cdot (\varepsilon^p)^{\hat{N}(\dot{\varepsilon}_*)+1} \right] \tag{7}$$

FITTING JCP TO THE SHPB AND INSTRON DATA

The total strains in Figure 3 were converted to plastic strains, ε_{xx}^p, by means of

$$\varepsilon_{xx}^p = \varepsilon_{xx} - \frac{\sigma_{xx}}{E} \tag{8}$$

E is Young's modulus. We estimated directly from the Instron curve in Figure 3 the value of 600 MPa for *E* at low strain rate. The criterion adopted was a 3% strain offset. No quantitive estimate for *E* could be made from the SHPB loading curves because equilibrium was not attained early in the test. We obtained the high-strain-rate estimate of 1.6 GPa for *E* based on unloading curves at the end of other SHPB tests. We applied equation 8 using 600 MPa for the Instron data and 1.6 GPa for the SHPB data, and obtained the stress-plastic strain data curves in Figure 4.

In the case of uniaxial stress σ_{xx} with all other components zero, the von Mises stress σ reduces to σ_{xx}.[5] If incompressibility is assumed, an increment $d\varepsilon^p$ of equivalent plastic strain reduces to $d\varepsilon_{xx}^p$, the plastic strain increment along the direction of uniaxial stress.[5] A similar argument can be used to reduce the equivalent total strain rate to the component along the direction of uniaxial stress.

The four SHPB tests in Figure 3 all involved an approximately constant strain rate of 2900/s. We treated these tests as constant-volume, adiabatic and applied equations 6 and 7 with $\dot{\varepsilon}_* = 2900/\mathrm{s}$. Initial temperature θ_i was either 297K or 325K. We obtained from reference 6 estimates of 2270 kg/m^3 for initial density ρ_0 and 1161 J/kg-K for specific heat c_v. We then applied the *FindFit* regression function in *Mathematica*[7] software to fit the constants $\hat{A}(2900/s)$, $\hat{B}(2900/s)$, $\hat{N}(2900/s)$, and θ_m. The results are contained in Table 1, and the JCP fit has been added to Figure 4.

The Instron data were obtained at a constant strain rate of 0.1/s. We again assumed constant volume and adiabatic conditions. (The latter assumption is less applicable here than it was for the SHPB data.) The value of 425K obtained for θ_m was carried over from the SHPB data analysis. Parameters $\hat{A}(0.1/s)$, $\hat{B}(0.1/s)$, and $\hat{N}(0.1/s)$ were evaluated by regression using *FindFit* of *Mathematica*[7]. The results are given in Table 2. The Instron fit has been added to Figure 4.

We chose 0.03/s for the normalizing strain rate $\dot{\varepsilon}_0$ because it is substantially smaller than the Instron strain rate of 0.1/s. Equation 2a, evaluated at strain rates of 0.1 and 2900/s, led to two linear algebraic equations for A_0 and A_1. Similarly, equation 2c produced two equations for N_0 and N_1. B_0 and B_1 were then evaluated directly from equation 2b. The resulting parameter values are contained in Table 3. The JCP yield strength could then be interpolated and extrapolated in terms of strain rate from its fits at 2900/s and 0.1/s.

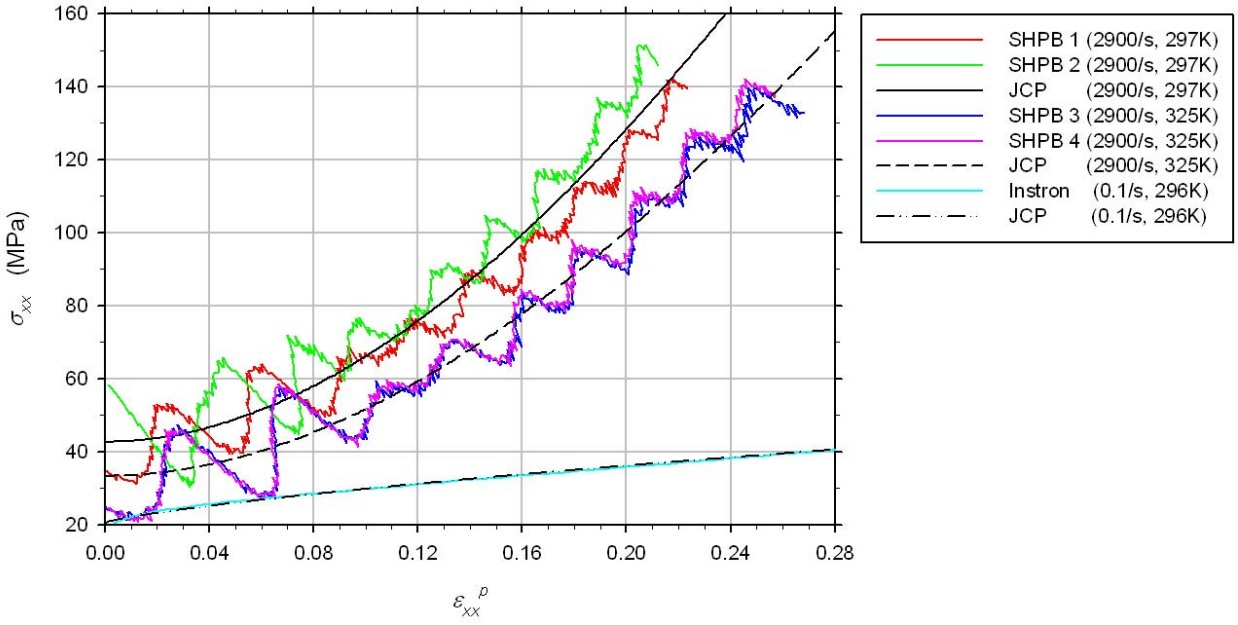

Figure 4. JCP Fits to SHPB and Instron Compression Data

Table 1. PTFE-Al Material Parameters Used in or Obtained From Fitting JCP to SHPB data

ρ_0 (kg/m^3)	c_v (J/kg-K)	E (GPa)	$\hat{A}(2900/\mathrm{s})$ (MPa)	$\hat{B}(2900/\mathrm{s})$ (GPa)	$\hat{N}(2900/\mathrm{s})$	θ_m (K)
2270	1161	1.6	43.71	1.998	1.901	425.3

Table 2. PTFE-Al Material Constants Used in or Obtained From Fitting JCP to Instron Data

ρ_0 (kg/m^3)	c_v (J/kg-K)	E (MPa)	$\hat{A}(0.1/\mathrm{s})$ (MPa)	$\hat{B}(0.1/\mathrm{s})$ (MPa)	$\hat{N}(0.1/\mathrm{s})$	θ_m (K)
2270	1161	600	20.83	57.34	0.7718	425.3

Table 3. JCP Material Constants for PTFE-Al

A_0 (MPa)	A_1 (MPa)	B_0 (MPa)	B_1	N_0	N_1	$\dot{\varepsilon}_0$ (1/s)	θ_m (K)
16.61	2.227	5.063	23.21	0.5633	0.1099	0.03	425.3

APPLICATION OF JCP TO THE SIMULATION OF TWO TAYLOR IMPACT TESTS

The JCP model was installed in the EPIC Lagrangian finite-element wavecode[4] and applied in simulations of two Taylor impact tests originally reported in reference 1. In reference 3 we previously simulated these tests using the Johnson-Cook yield strength model[8], and we here re-visited them applying JCP. Both rods had initial length and radius of 50.8 and 7.59 mm, respectively. They were modeled using axisymmetric, 4-node quadrilaterals with single-point integration and an initial element size of 0.1 mm. The aluminum sabot was represented by concentrated masses distributed along the boundary of the rearmost 10 mm of the rod. The steel anvil was modeled as rigid, and its interface with the rod as frictionless. The dilatational behavior of PTFE-Al was modeled with the Mie-Grüneisen equation of state representation adopted in reference 6. The shock Hugoniot was represented by a linear shock speed-particle speed relationship. In reference 6 an intercept of 1450 m/s and slope of 2.258 were obtained directly from shock-Hugoniot data. The constant Grüneisen parameter was estimated to be 0.9. The elastic shear modulus was 554 MPa, which we determined from the high-rate Young's modulus of 1.6 GPa, and the elastic bulk modulus consistent with the 1450-m/s intercept of the shock Hugoniot.

Figure 5 shows the computed rod shapes for 104-m/s impact superimposed on the boundary locations digitized from framing-camera photographs. Note that radial displacements have been amplified by a factor of 5 in this figure. The EPIC simulations agree reasonably well in terms of the rod's shape versus time. The final outer radius at the anvil interface is in particularly close agreement.

Figure 6 shows computed contours of equivalent plastic strain and temperature at 36 μs after impact at 104 m/s. Note the conical shape of these contours. If we adopt the hypothesis that an ignition criterion should be based on equivalent plastic strain ($\varepsilon^p_{\mathrm{ign}}$), then the conical contours in Figure 6 support our earlier speculation that ignition first occurred on the surface of the recovered specimen in Figure 2.

Figure 7 compares with experiment the computed specimen shape for various times after 222-m/s impact. (Radial displacements are not multiplied by 5 as they are in Figure 5.) The computed shape shows good agreement with experiment at 4, 8, 12, and 16 μs after impact. By 20 μs, however, the mushroomed volume is substantially larger in the experiment than in the calculation. This discrepancy between theory and experiment becomes successively more pronounced at 24, 28, and 32 μs.

Thus, at an impact speed of 222 m/s, the EPIC simulation under-predicts the extent of mushrooming at 20, 24, 28, and 32 μs but not at 4, 8, 12, and 16 μs. Several explanations can be envisioned. First, the JCP fit might not apply throughout the ranges of strain, strain rate, and temperature that the Taylor rod underwent in the course of the test. Specifically, the fit was interpolated in terms of strain rate and temperature and extrapolated in terms of strain, strain rate and temperature. Second, there may have been fracture and associated void formation within the rod. Third, there may have been interior ignition and associated gas formation.

DIRECT OBSERVATIONS OF PETALLING

Figure 8 contains photographs from a modified Taylor impact test, using a small-diameter steel anvil. The PTFE-Al rod's initial length and diameter were 25.4 mm and 6.4 mm, respectively. The anvil's diameter was 9.5 mm. The impact speed was 202 m/s. The photograph at 50 μs clearly displays the failure mode known as "petalling", which refers in this case to radial cracks in the mushroomed region. Petalling involves tensile failure. In the mushroomed region, the rod undergoes progressive circumferential tension, eventually leading to rupture.

CRITICAL STRAIN FOR SHEAR LOCALIZATION; IMPLICATIONS FOR IGNITION

In Figure 10, we have extrapolated to larger strain values the JCP fit in Table 1. The JCP fit, evaluated for either initial temperature, attains its maximum value at an equivalent plastic strain, ε_c^p, of 0.66. As strain is increased above ε_c^p, the decrease in σ_{JCP}^{adiab} due to thermal softening has a larger magnitude than the increase due to strain hardening. The resulting negative slope in the adiabatic stress-strain curve at strains greater than ε_c^p can lead to the phenomenon of shear localization such as occurs in certain metals. The material is locally unable to equilibrate its load. Additional plastic flow generates an additional temperature rise, which further softens the material. A self-sustaining process develops which leads to the local state of zero deviatoric stress and the plateau value of θ_m for temperature. Temperature as a function of strain is given by equation 5 and has been added to Figure 10.

The shear localization phenomenon may have an added significance in the case of PTFE-Al, with its potential for ignition. We speculate that the concentrated shearing motion may be able to strip the oxide layer from aluminum particles in the shear band, thereby exposing those particles to the surrounding PTFE. Perhaps such exposure is a necessary condition for ignition.

The critical strain ε_c^p is defined by

$$\left.\frac{d\sigma_{JCP}^{adiab}(\varepsilon^p,\dot{\varepsilon}_*)}{d\varepsilon^p}\right|_{\varepsilon^p=\varepsilon_c^p} = 0 \tag{9}$$

Substitution of equation 6 into 9 yields the algebraic equation

$$(\varepsilon_c^p)^{2\hat{N}} + \frac{2\hat{A}}{\hat{B}}(\varepsilon_c^p)^{\hat{N}} - \frac{\hat{N}\rho_0 c_v(\theta_m - 294\mathrm{K})}{\hat{B}}(\varepsilon_c^p)^{\hat{N}-1} + \left(\frac{\hat{A}}{\hat{B}}\right)^2 = 0 \tag{10}$$

The coefficients of this equation involve $\hat{A}$, $\hat{B}$, and $\hat{N}$, which are functions of strain rate. It follows that the solution for ε_c^p is also a function of strain rate. Hence, if ignition is initiated by shear localization, we expect that the value of strain corresponding to ignition initiation, call it $\varepsilon_{\mathrm{ign}}^p$, is a function of strain rate. Moreover, the physical processes that intervene between shear localization and ignition can introduce additional time scales and thereby make $\varepsilon_{\mathrm{ign}}^p$ more strongly dependent on strain rate than is ε_c^p. These processes include the mechanical stripping of the aluminum particles' oxide layer and startup of the chemical reaction(s).

A MODEL FOR PARTIAL EFFECTS OF IGNITION

A model that introduces into a PTFE-Al impact simulation some effects of ignition was added to EPIC to use in conjunction with JCP yield strength. This ignition effects model introduces three material constants: ignition strain, $\varepsilon_{\mathrm{ign}}^p$, potential chemical energy per unit mass, e_0, and the time duration of the chemical reaction, Δt_{ign}. The model consists of two parts: a criterion for detecting ignition and a post-

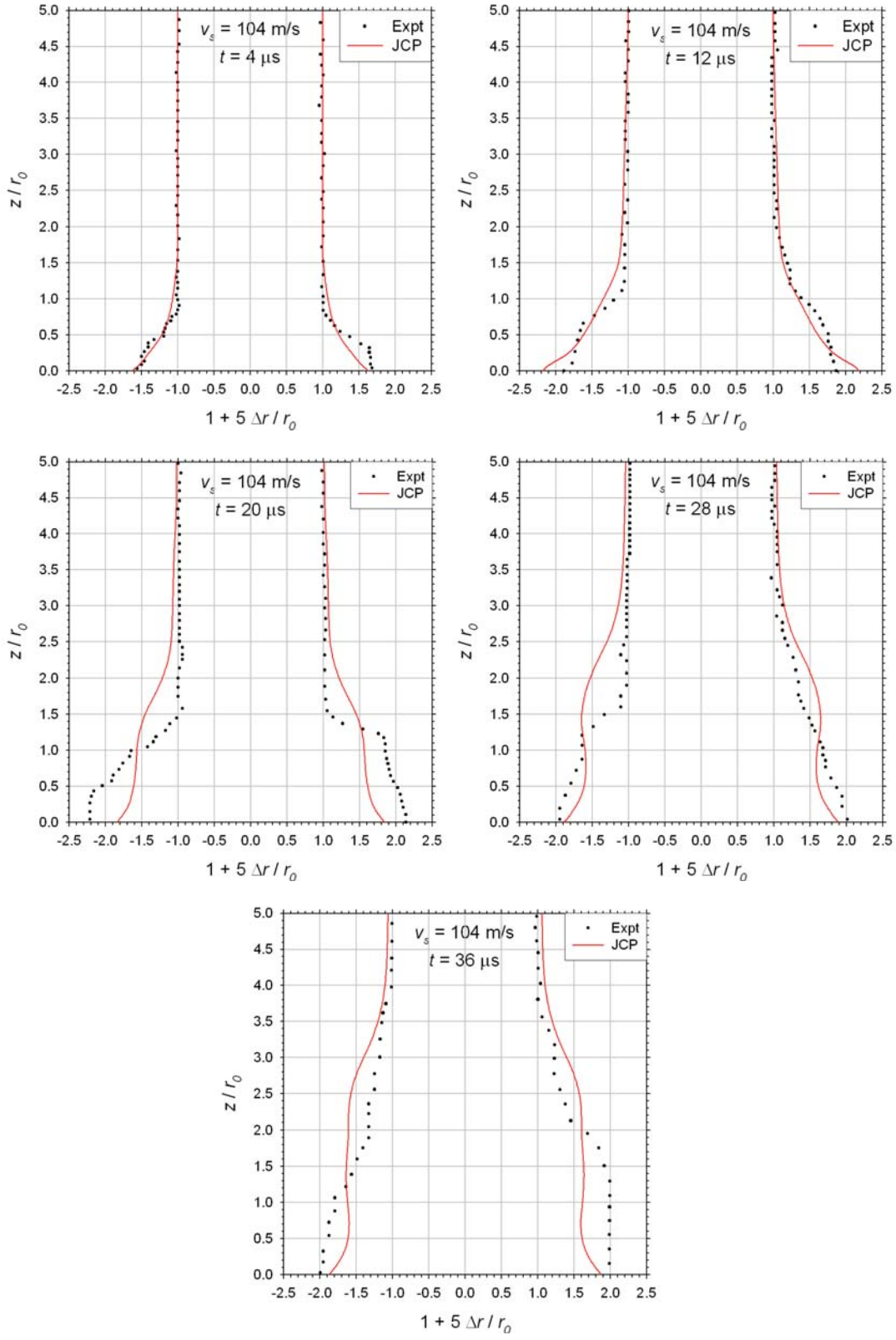

Figure 5. Experimental and computed specimen boundaries in the Talyor impact test at an impact speed of 104 m/s. (Experimental data reproduced from reference 3.)

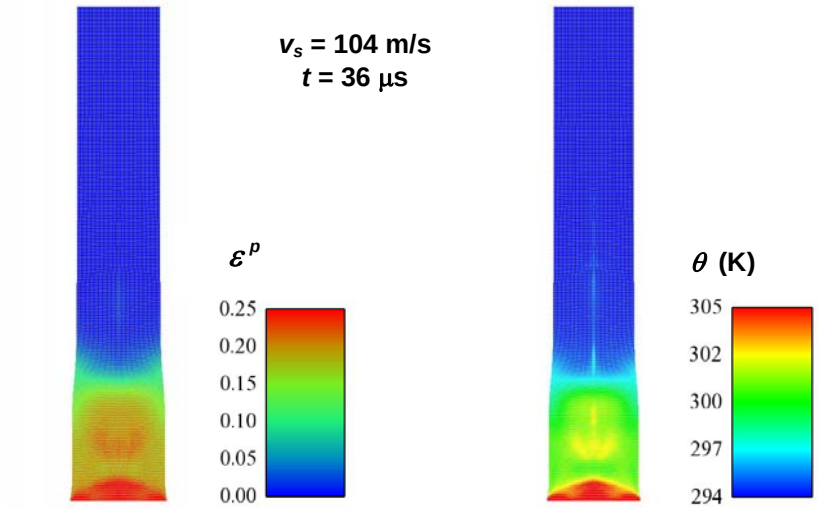

Figure 6. Contours of equivalent plastic strain and temperature at 36 μs after impact at 104 m/s.

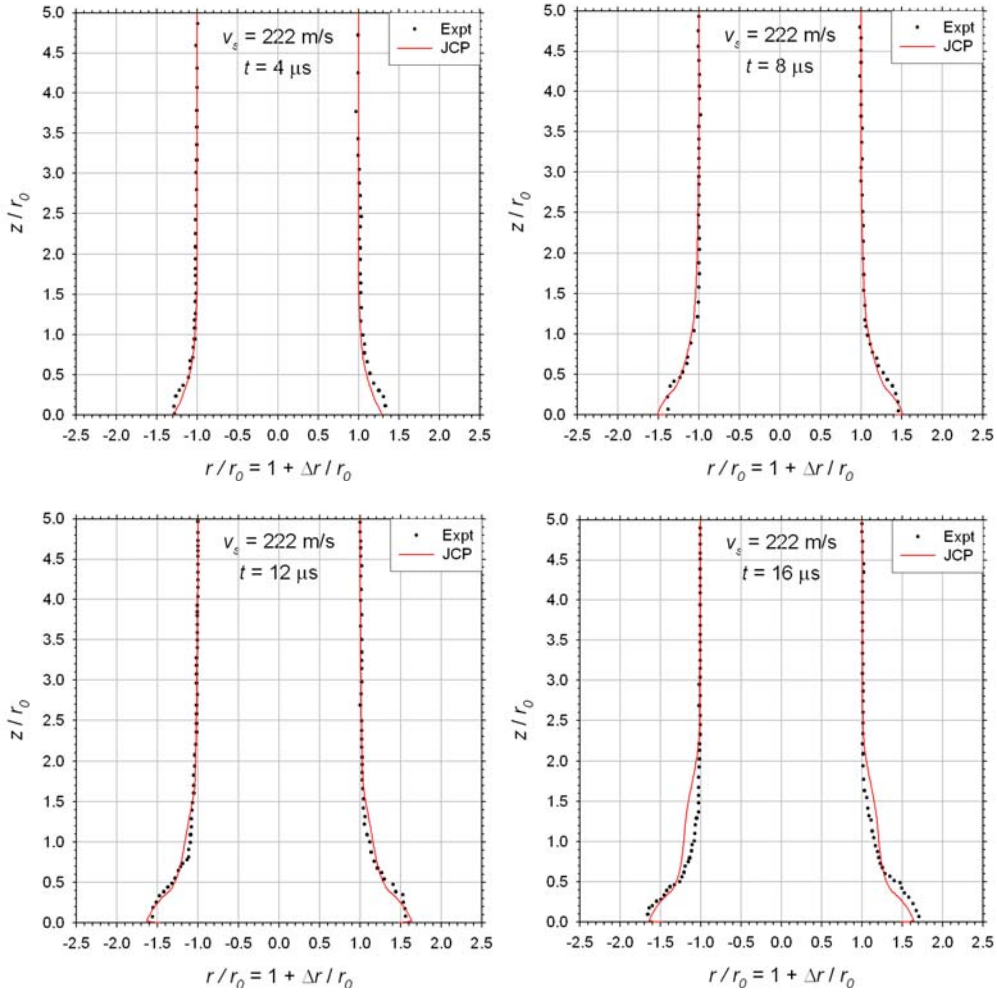

Figure 7a. Experimental and computed specimen boundaries in the Taylor impact test at an impact speed of 222 m/s (4, 8, 12, and 16 μs after impact). (Experimental data reproduced from reference 3.)

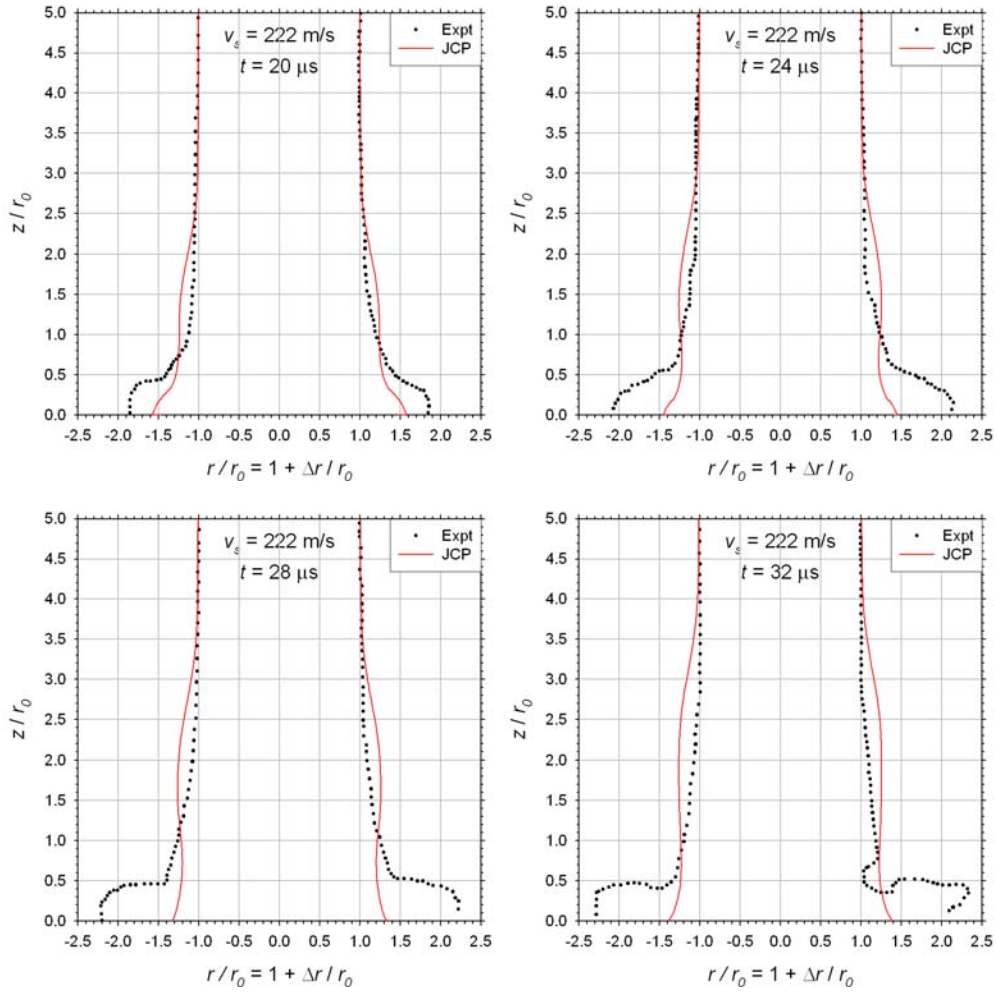

Figure 7b. Experimental and computed specimen boundaries in the Taylor impact test at an impact speed of 222 m/s (20, 24, 28, and 32 μs after impact). (Experimental data reproduced from reference 3.)

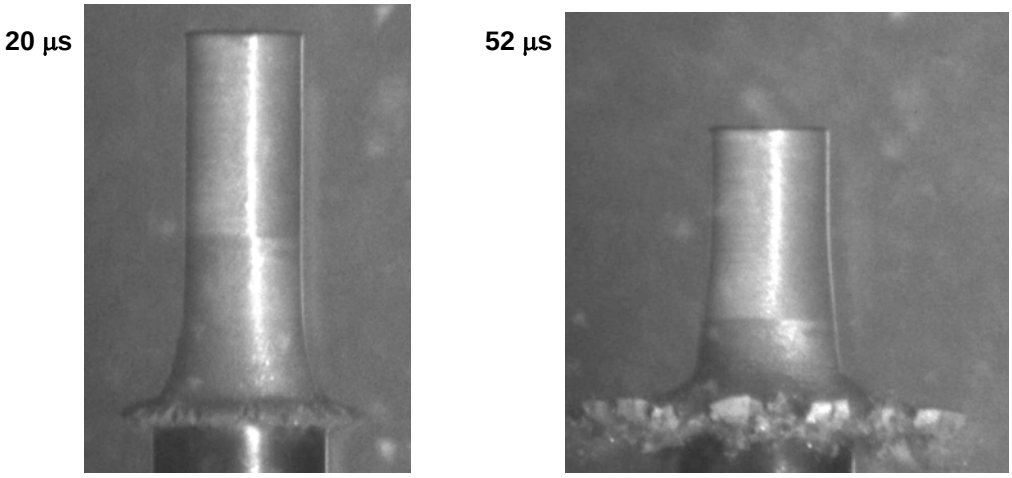

Figure 8. A modified Taylor impact test with an PTFE-Al specimen impacting at 202 m/s a small-diameter steel anvil. Petalling fracture has begun by 20 μs and is pronounced at 52 μs.

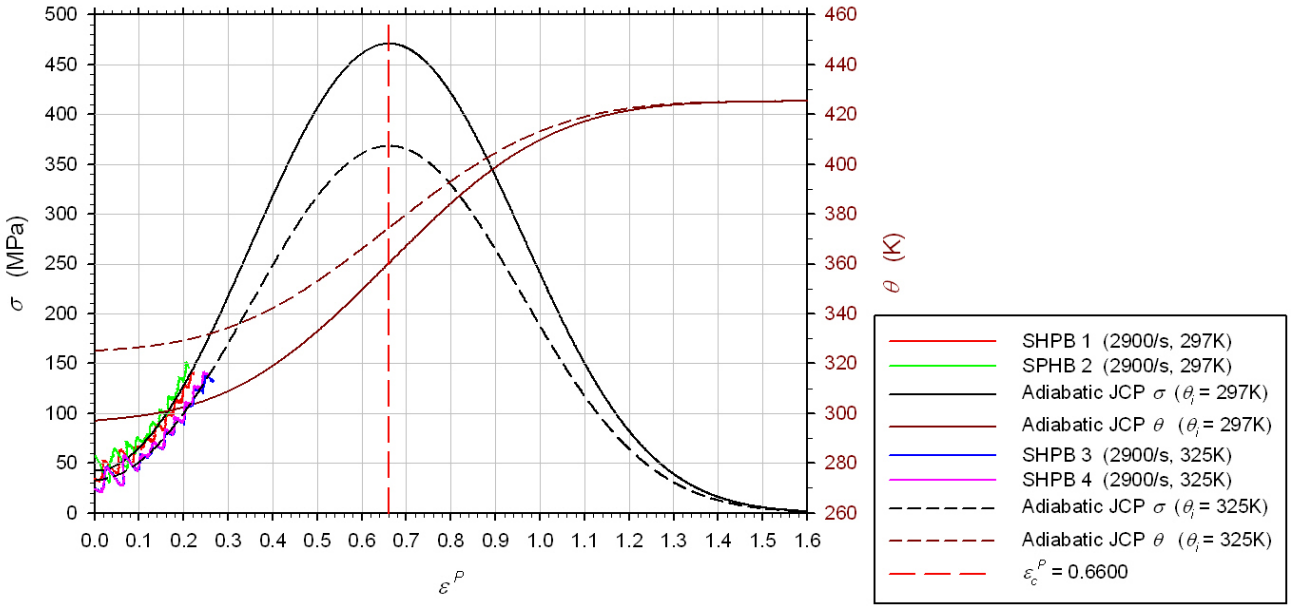

Figure 10. The JCP Fit at $\dot{\varepsilon} \equiv 2900/s$, Extrapolated to Larger Values of Strain. Note the Critical Strain of 0.66 Corresponding to Maximum Stress.

detection algorithm. The detection criterion, applied individually to each finite element, is

$$\varepsilon^p \geq \varepsilon^p_{\text{ign}} \tag{11}$$

The element-dependent parameter t_{ign} is the time associated with the time step at which equation 11 was first satisfied within that element. The element's increment in specific internal energy (per unit mass) is computed for a given time step of duration Δt at time t using

$$\Delta e_{\text{ign}} = \begin{cases} 0 & ; \quad t < t_{\text{ign}} \\ e_0 \cdot \dfrac{\Delta t}{\Delta t_{\text{ign}}} & ; \quad t_{\text{ign}} \leq t \leq t_{\text{ign}} + \Delta t_{\text{ign}} \\ 0 & ; \quad t_{\text{ign}} + \Delta t_{\text{ign}} < t \end{cases} \tag{12}$$

Δe_{ign} is identified with the increment in specific internal energy generated by the chemical reaction.

The post-detection algorithm applies Δe_{ign} as a source term in the first law of thermodynamics,

$$\rho_0 c_v \Delta\theta = \sigma_{\text{JCP}}(\varepsilon^p, \theta, \dot{\varepsilon})\,\Delta\varepsilon^p \; + \; \Delta e_{\text{ign}} \tag{13}$$

and in the Mie-Grüneisen equation of state,

$$P(\rho, e) = \frac{\rho_0 {c_0}^2 S\eta}{(1 - S\eta)^2}\left(1 - \frac{\Gamma\eta}{2}\right) \; + \; \Gamma\rho_0 \,(e \; + \; \Delta e_{\text{ign}}) \tag{14}$$

In equation 11 $\Delta\theta$ and $\Delta\varepsilon^p$ are the increments in temperature and equivalent plastic strain, respectively, in that element during the given time step. In equation 12, $\eta = 1 - \rho_0/\rho$, where ρ is the current density within the element.

Equation 11 contains the assumptions that the process is effectively adiabatic and that the energy increment associated with the material's density change is negligible relative to the increments in plastic work and chemical energy. According to equation 11, the introduced chemical energy raises the element's temperature. This reduces the element's yield strength by equation 1. In a Taylor impact simulation, a result would tend to be an increased mushrooming. According to equation 12, the introduced chemical energy is accompanied by a rise in pressure. This would produce an increased specific volume and also tend to lead to an increased mushrooming.

The model ignores a known effect of ignition, namely the material's phase change into gaseous products. At a given time following the local onset of ignition, the material within a lagrangian finite element should be divided between a certain volume fraction still in the solid phase and the remaining volume fraction converted to a gas. Equations 13 and 14 should properly only apply to the material still in the solid phase.

SUMMARY AND CONCLUSIONS

The JCP model was developed to relate the von Mises yield strength of a reactive PTFE-aluminum composite to equivalent plastic strain, total strain rate, and temperature. The model was fit to Instron and SHPB compression data at strain rates of 0.1/s and approximately 2900/s, respectively. The model was installed into the EPIC finite element wavecode and used to simulate Taylor impact tests at impact speeds of 104 and 222 m/s. The rods' initial length and diameter were 50.8 and 7.59 mm, respectively. The computed boundary shapes versus time were compared with digitized images from a framing camera. Agreement was good at 104 m/s throughout the observed 36-μs duration. At 222 m/s, agreement was good until 16 μs after impact. Thereafter the photographs displayed a greater degree of mushrooming than did the EPIC simulation. Our speculated reasons for this under-predicted late-time mushrooming included inaccuracies introduced by extrapolations and/or interpolations of our JCP fit, material fracture, and ignition. The fracture hypothesis was then supported in a modified Taylor impact test in which petalling fracture was observed by means of a higher resolution camera.

A model was developed to introduce partial effects of ignition into an EPIC simulation. The ignition criterion is based on a critical value of equivalent plastic strain. After detection, effects of the chemical reaction are introduced by means of a source term in the first law of thermodynamics and in the Mie-Grüneisen equation of state. The model is partial in that transformation into gaseous products has not yet been taken into account. This model should be refined and then applied in Taylor impact simulations. A model for petalling fracture is also required for a more complete Taylor impact simulation.

REFERENCES

1. Mock, W., and Holt, W. H., Impact initiation of rods of pressed polytetrafluoroethylene (PTFE) and aluminum powders, ***Shock Compression of Condensed Matter - 2005***, editors: Furnish, M. D., Elert, M., Russell, T. P., White, C. T., American Institute of Physics, Melville, NY, 2006, pp. 1097-1100.
2. Casem, D. A., and Raftenberg, M. N., Initiation experiments on Aluminum/PTFE, ***Proceedings from the 41st JANNAF Combustion Subcommittee Meeting***, San Diego, 2006.
3. Raftenberg , M. N., Mock, W., Jr., and Kirby, G. C., Modeling the impact deformation of rods of a pressed PTFE/Al composite mixture, ***International Journal of Impact Engineering***, in press.
4. Johnson, G. R., Colby, D. D., and Vavrick, D. J., Three dimensional computer code for dynamic response of solids to intense impulsive loads, ***International Journal of Numerical Methods in Engineering***, vol. 14, 1979, pp. 1865-1871.
5. Malvern, L. E., ***Introduction to the Mechanics of a Continuous Medium***, Prentice-Hall, Englewood Cliffs, NJ, 1969, p. 364.
6. Taylor, P. A., ***CTH Reference Manual: The Pressure Shear Damage (PSDam) Model***, SAND2003-0539, March 2003.
7. *Mathematica* 6.0, http://www.wolfram.com.
8. Johnson, G. R., Cook, W. H., A constitutive model and data for metals subjected to large strains, high strain rates and high temperatures, ***Proceedings from the 7th International Symposium on Ballistics***, 1983, pp. 541-547.

NO. OF
COPIES ORGANIZATION

1 (PDF ONLY) DEFENSE TECHNICAL INFORMATION CTR
DTIC OCA
8725 JOHN J KINGMAN RD
STE 0944
FORT BELVOIR VA 22060-6218

1 US ARMY RSRCH DEV & ENGRG CMD
SYSTEMS OF SYSTEMS INTEGRATION
AMSRD SS T
6000 6TH ST STE 100
FORT BELVOIR VA 22060-5608

1 DIRECTOR
US ARMY RESEARCH LAB
IMNE ALC IMS
2800 POWDER MILL RD
ADELPHI MD 20783-1197

1 DIRECTOR
US ARMY RESEARCH LAB
AMSRD ARL CI OK TL
2800 POWDER MILL RD
ADELPHI MD 20783-1197

1 DIRECTOR
US ARMY RESEARCH LAB
AMSRD ARL CI OK T
2800 POWDER MILL RD
ADELPHI MD 20783-1197

ABERDEEN PROVING GROUND

1 DIR USARL
AMSRD ARL CI OK TP (BLDG 4600)

NO. OF COPIES	ORGANIZATION
1 (CD ONLY)	JOINT DOD/DOE MUNITIONS DEV PRGM E BROWN 3090 DEFENSE PENTAGON RM 5C756 WASHINGTON DC 20301-3090
9	NSWC DAHLGREN DIV W MOCK JR J DROTAR B MYRUSKI J SHULTIS W CHEPREN M HOPSON L WILSON R GARRETT D DICKINSON 17320 DAHLGREN RD DAHLGREN VA 22448-5100
1	NAVAL RESEARCH LAB G KIRBY CODE 8221 SYS ANLYS BR WASHINGTON DC 20375
6	AIR FORCE RSRCH LAB MUNITIONS DIR W RICHARDS J JORDAN M DENIGAN Y HORIE L CHHABILDAS M KRAMER EGLIN AFB FL 32542
1	US ARDEC J PHAM BLDG 65S PICATINNY ARSENAL NJ 07806-5000
1	US ARDEC AMSRD AAR AEM T M NICOLICH BLDG 65 S PICATINNY ARSENAL NJ 07806-5000
1	US ARDEC AMSRD AAR AEP E D CARLUCCI BLDG 94 PICATINNY ARSENAL NJ 07806-5000

NO. OF COPIES	ORGANIZATION
6	LOS ALAMOS NATIONAL LAB B CLEMENTS T MASON D DATTELBAUM P REA E MAS F ADDESSIO PO BOX 1663 LOS ALAMOS NM 87545
6	SANDIA NATIONAL LABS M BAER R SCHMIDT E HERTEL P TAYLOR T VOGLER TECH LIB PO BOX 5800 ALBUQUERQUE NM 87185-5800
3	DIRECTOR LAWRENCE LIVERMORE NATIONAL LAB D GOTO T ORZECHOWSKI JOHN REAUGH L-32 PO BOX 808 LIVERMORE CA 94550
3	SOUTHWEST RSRCH INST G R JOHNSON T J HOLMQUIST S BEISSEL 5353 WAYZATA BLVD STE 607 MINNEAPOLIS MN 55416
3	SOUTHWEST RSRCH INST ENGR DYNAMICS DEPT C E ANDERSON J WALKER K DANNEMANN PO BOX 28510 6220 CULEBRA RD SAN ANTONIO TX 78228-0510
1	RAYTHEON MISSILE SYSTEMS R AMES 1151 HERMANS RD TUCSON AZ 85706

NO. OF COPIES ORGANIZATION

1 DYNA EAST CORP
W FLIS
3620 HORIZON DR
KING OF PRUSSIA PA 19406-2647

1 INTERNATIONAL RSRCH ASSOC
D L ORPHAL
4450 BLACK AVE
STE E
PLEASONTON CA 94566

2 INST FOR ADVANCED TECHLGY
S BLESS
S SATAPATHY
3925 W BRAKER LN
AUSTIN TX 78759-5316

1 DEFENSE THREAT REDUCTION AGCY
K KIM
8725 JOHN KINGMAN RD
FT BELVOIR VA 22060-6201

1 APPLIED RSRCH ASSOC
D GRADY
4300 SAN MATEO BLVD NE
STE A 220
ALBUQUERQUE NM 87110

1 LIVERMORE SOFTWARE TECHLGY CORP
J HALLQUIST
7374 LAS POSITAS RD
LIVERMORE CA 94550

1 PURDUE UNIV
AERONAUTICS AND ASTRONAUTICS
W CHEN
GRISSON HALL RM 376
315 N GRANT ST
WEST LAFAYETTE IN 47907-2023

1 UNIV CINCINNATI ENGRG
A TABIEI
787 RHODES HALL
CINCINNATI OH 45221-0070

NO. OF COPIES ORGANIZATION

1 NARESH N THADHANI
GEORGIA INST OF TECHLGY
MATERIALS SCI AND ENGRG
771 FERST DR NW
ATLANTA GA 30332-0245

1 VIRGINIA POLYTECH INST
ENGRG SCIENCE
R BATRA
BLACKSBURG VA 24061-0219

1 NORTHWESTERN UNIV
MECHL ENGRG
W K LIU
EVANSTON IL 60208

1 UNIV ALABAMA
ENGRG MECHANICS
S E JONES
PO BOX 870278
TUSCALOOSA AL 34587-0278

1 UNIV MISSOURI ROLLA
CIVIL ENGRG
W SCHONBERG
ROLLA MO 65409-0030

1 UNIVERSITY ALABAMA
MECHL ENGRG
D LITTLEFIELD
HOEN 330A
BIRMINGHAM AL 35294-4440

2 JOHNS HOPKINS UNIVERSITY
MECHANICAL ENGRG
K T RAMESH
K HEMKER
LATROBE HALL
BALTIMORE MD 21218-2689

2 DIR ARMY RSRCH OFC
A RAJENDRAN
B LAMATTINA
PO BOX 12211
RESEARCH TRIANGLE PARK
NC 27709-2211

NO. OF
COPIES ORGANIZATION

ABERDEEN PROVING GROUND

42 DIR USARL
AMSRD ARL WM
R DOWDING
J MCCAULEY
S MCKNIGHT
J SMITH
AMSRD ARL WM B
J NEWILL
AMSRD ARL WM BD
B FORCH
B HOMAN
K MCNESBY
AMSRD ARL WM MB
D HOPKINS
L KECSKES
AMSRD ARL WM MD
B CHEESEMAN
E CHIN
G GAZONAS
C RANDOW
C YEN
AMSRD ARL WM T
P BAKER
AMSRD ARL WM TB
R BANTON
R BITTING
W BUKOWSKI
N ELDREDGE
R GUPTA
S KUKUCK
AMSRD ARL WM TC
T FARRAND
L MAGNESS
D SCHEFFLER
B SCHUSTER
S SEGLETES
AMSRD ARL WM TD
S BILYK
T BJERKE
D CASEM
J CLAYTON
Y HUANG
R KRAFT
B LOVE
M RAFTENBERG (5 CPS)
M SCHEIDLER (2 CPS)
T WEERASOORIYA